Electrochemical characteristics of Si/Mo multilayer anode for Li ion batteries

Myung-Hoon Kim[a], Young-Jae Kim[a], Jung-Yeul Kim[b], You-Ki Lee[b], J.A. Ascencio[c], and Jong-Wan Park[a,*]
[a]*Division of Materials Science and Engineering, Hanyang University,*
17 Haengdang-Dong, Seongdong-Gu, Seoul 133-791, Korea.
[b]*Division of Semiconductor and Electronics Engineer, Uiduk University,*
50 Yukum-Li Kangdong-Myun, Kyoungju-Si, Koungsangbuk-Do, 780-713 Korea.
[c]*Programa de Investigación y Desarrollo de Ductos, Instituto Mexicano del Petróleo.*
e-mail: myung97@ihanyang.ac.kr, kim0jae@ihanyang.ac.kr,
jykim@uu.ac.kr, leeyk@uu.ac.kr, jascencio@yahoo.com

We have prepared the Si/Mo multilayer by alternate deposition with a multi-gun rf/dc magnetron sputtering system. A current collector was Cu foil that had a rough surface. Pre-treatment with plasma on the surface was performed in order to improve adhesion between an electrode and substrate and to remove contamination on the surface. The structural and electrochemical characteristics of yhe Si/Mo multilayer were investigated. The initial capacity of the Si thin film rapidly degraded after 40 cycles, whereas the multilayer maintained more than 90 % of the initial capacity (2653 mAhg^{-1}) after 100 cycles.

Keywords: Silicon; molybdenum, multilayer; anode; Li ion secondary battery.

Se prepararon las múltiples capas de Si/Mo por deposición alternada mediante un sistema de erosión catódica de magnetrón rf/dc de múltiples cañones. Un colector de corriente era la lámina de Cu de superficie áspera. Se realizó el pre-tratamiento con plasma en la superficie para mejorar la propiedad de adherencia entre electrodo y sustrato y para eliminar contaminación de la superficie. Se investigaron las características estructurales y electroquímicas de las multicapas de Si/Mo. La capacidad inicial de la película delgada de Si degradó rápidamente después de 40 ciclos mientras que las multicapas mantuvieron más del 90% de la capacidad inicial (2653 mAhg-1) después de 100 ciclos.

Descriptores: Silicio; molibdeno; multicapas; ánodo; batería secundaria Li-ion.

PACS: 82.45.-h; 82.47.Aa

1. Introduction

Graphitized carbon has been used as the anode material for commercial lithium-ion batteries. Although graphite has many merits– low and flat working voltage, small volumetric change and good cycle performance– it cannot satisfy the demands of a high energy density lithium-ion battery for portable electric devices because of its restricted theoretical capacity (LiC_6, gravimetric capacity of 372mAh/g, volumetric capacity of 830Ah/L)[1,2]. Also, the capacity of commercial graphite has been improved and almost has recently reached the level of its theoretical capacity.

As an alternative anode material with a higher capacity, lithium alloys, *e.g.* $Li_xM(M = Sn, Si, Ge, Al, etc)$ have attracted the attention of many research groups[19-21]. Despite the interesting performance of high lithium packing density and safe thermodynamic potentials compared with carbonaceous materials, the alloys involve a major problem: considerable expansion/contraction during the charging/discharging processes. The alloy electrodes are gradually deformed with repeating cycles. This is a main drawback for their use as an anode material in lithium-ion batteries.

Si can react with lithium to form alloys with a high Li/Si ratio[3]. Electrochemical Li-Si reaction occurs between 0 and 0.3 V against Li/Li$^+$, so that the battery can have high-energy density. In the case of $Li_{22}Si_5$, the theoretical capacity corresponds to 4200mAh/g. Si undergoes, however, greater volume change than any other alloy material during lithium insertion and extraction. The large volume difference between the lithiated host and the lithium-free host– $Li_{4.4}Si$ is up to four times larger than for Si– causes cracking and crumbling of the Si particles. It leads to morphological changes and loss electrical contact loss between the host material and the current collector. Thus, the capacity of silicon alloy on cycling has been fading rapidly [4].

The research groups of Huggins [5,6] and Besenhard [7] have proposed that the volume expansion due to the insertion of lithium can be reduced in micro- and submicro-structured matrix alloys. The composite materials are made of both active nano-grains, which react with lithium, and an inactive matrix incapable of alloy formation with lithium. For example, silicides such as Cr-Si [8], Ni-Si [9], TiN-Si [10] and Mg_2Si [11-13] have been researched.

Their improved cycle ability was suggested from the role of the inactive matrix, which buffers the volumetric change of the Si phase and provides a good connection for electrical or ionic conduction during lithium insertion and extraction processes. The research into mechanical alloying by high-energy ball mill has focused on reducing the particle size of the host material and using multi-phase materials or intermetallic compounds. Although these solutions are desirable, they would not solve the main problems, which related to the large irreversible capacity due to electrolyte decomposition affecting the formation of solid electrolyte interface (SEI) films and the pulverization of active material.

Therefore, it is necessary to develop a material system that can definitely reduce the mechanical stress and volume change related to the alloying process between Li and Si. As an example, Yoshio *et al.* reported that carbon-coated Si prepared by a thermal vapor decomposition (TVD) achieved the capacity of 980 mAh/g stably up to 20 cycles[14].

In thin film deposition techniques, the multilayer structure can be prepared more properly than the composite material since these techniques offer a certain control of the grain size in the direction of growth at least. The film's characteristics are closely related to the microstructure of the multilayer such as the each layer's thickness, the number of multilayer period, the ratio of the active/inactive elements, the degree of interface perfection, and the selection of materials.

The fundamental notation of active/inactive multilayer is that the active layer is sandwiched between two inactive layers. This inactive layer led to an effective buffer to relieve the stress because of the change in volume during cycling. It can be achieved by magnetron sputtering [15] and electron beam evaporation[16].

Inactive metal incapable of alloy formation with lithium include Ca, Cu, Cr, Mg, Mn, Mo, Nb, Ni, Ta, Ti, V, Fe, Co, and the like. The factors such as the strong affinity between inactive material and Si, the formation of a mixed layer or an intermetallics compound via diffusion of an element constituent and high electrical conductivity of inactive material due to low electrical conductivity of Si must be considered for the selection of promising inactive material. Thus, among these inactive elements, Mo is particularly preferred in this study.

In this study, we investigated sequentially deposited Si/Mo multilayer. At first, the study discusses the structural properties of multilayer (stacking) and then mentions the electrochemical characteristics of the film as an anode in lithium-ion batteries.

2. Experimental

Si and Mo layers were deposited alternately with a fixed periodicity and a desired thickness by rf/dc magnetron sputter with multi-target system. The chamber was evacuated down to 3.0×10^{-6} Torr as a base pressure. A working pressure of 5 mTorr was maintained with argon gas. In order to obtain an accurate deposition, a shutter is introduced between the substrate and the target. Si/Mo multilayer thin film was fabricated sequentially depositing 120 times of each Si sublayer and Mo sublayer. Therefore, the film was composed of a total of 240 layers. The thickness of each sublayer is monitored by the deposition time. Si sublayer in each layer was deposited for 30 s. Deposition time of Mo sublayer in each layer was adjusted from 3 s to 12s in order to change the thickness of Mo. In order to identify the advantages of multi-phase employing an inactive element, Si monolayer film was deposited as a comparative specimen and the thickness of the film was similar to the total Si sublayer of multilayer.

The films were deposited on an electrolytic Cu foil having an arithmetic mean roughness (Ra) of 0.5 μm (about 18 μm thick) for electrochemical analysis. Before the deposition of thin film, the current collector is subjected to a plasma treatment as a pre-treatment for removing surface contamination. The plasma treatment was performed by generating an ECR plasma in a separately installed plasma generator and irradiating the surface of the substrate in a reaction chamber.

The deposited multilayers were characterized by using cross-sectional transmission electron microscopy (TEM, JEOL2010). Structural identification of Si thin film and multilayer was primarily conducted by x-ray diffractometry (RINT 2000, RIGAKU) with Cu Kà radiation and Raman spectroscopy. Also, the mass of Si and Mo elements was analyzed by using an inductively coupled plasma (ICP) mass spectrometer. The morphologies of sample were observed using a scanning electron microscope(FE-SEM).

The electrochemical measurements were conducted with a typical two-electrode coin-type cell (CR2032, Hohsen Co. Ltd., Japan). The coin type cell was composed of a lithium metal (= anode) as both the counter electrode and reference electrode, porous polyethylene film as separator and deposited film (= cathode) as a working electrode. The electrolyte was a 1:1 v/v mixture of ethylene carbonate (EC) and diethyl carbonate (DEC) containing 1M LiPF$_6$ (Merck). The cell was assembled and sealed in an argon filled dry box. The charge-discharge measurements with a cycle tester (WBCS 3000, WON A TECH) were carried out between 0.01 and 1.0 V potential range. Lithium ions inserted into and extracted from deposited films are defined as discharge and charge processes, respectively.

3. Results and Discussion

Figure 1 shows the XRD peaks of each film. No diffractions except those of the Cu substrate (JCPDS 03-1005) were
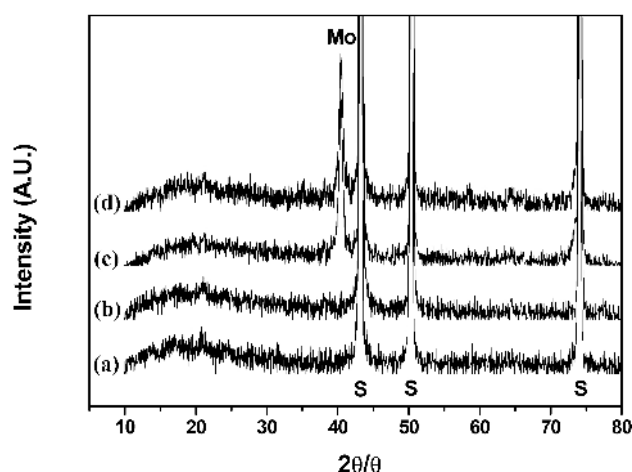
FIGURE 1. XRD patterns of (a) Cu foil, (b) a-Si thin film on a Cu foil, (c) Mo thin film on a Cu foil, (d) Si/Mo multilayer on a Cu foil ('S' denotes substrate).
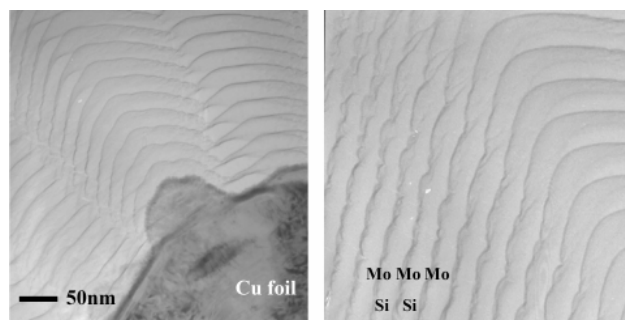
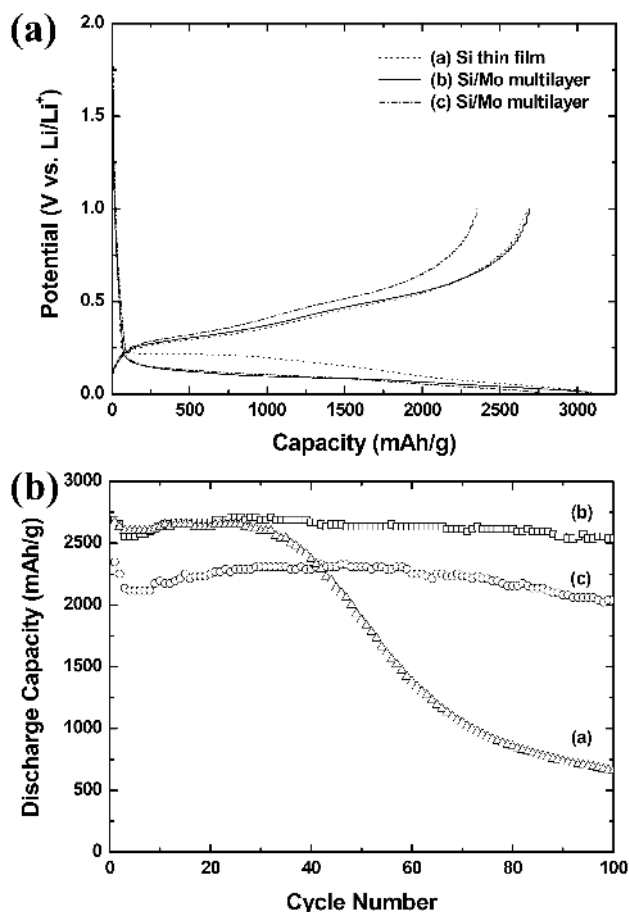FIGURE 2. Cross-sectional TEM image of the Si/Mo Multilayer on Cu foil.

FIGURE 3. (a) Initial charge-discharge curves and (b) the specific discharge capacity vs. cycle number of the Si thin film and Si/Mo multilayer. Electrode potential range 0.01-1.0 V vs. Li/Li$^+$; charge-discharge current density 0.55 mAcm^{-2}. (a) the Si thin film, (b) the Si/Mo multilayer of 120 layers (Si layer : 26 nm, Mo layer : 3 nm) , (c) the Si/Mo multilayer of 120 layers (Si layer : 26 nm, Mo layer : 10 nm).
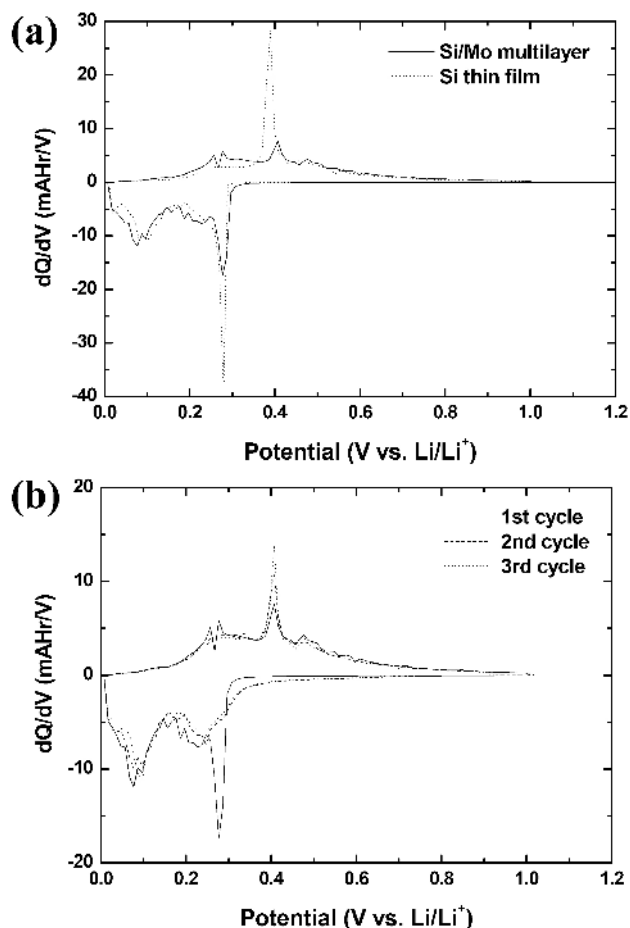

FIGURE 4. Differential capacity plots of (a) the first cycle of Si thin film and Si/Mo multilayer and (b) the first three cycles of Si/Mo multilayer.

detected by the XRD patterns of Si thin film. Raman spectroscopy detected only the substantial presence of a peak around 480cm^{-1} corresponding to an amorphous region [17]. Therefore, we suppose that the deposited Si thin film had the amorphous phase. However, the Mo thin film (JCPDS 42-1120) had a small peak to be related to fine crystallite of Mo (110) at 40.45°. The peak of Mo (200) at 58.8° was not detec-

ted and that of Mo (211) at 73.7° was overlapped the Cu (220) peak at 74.0°. The Si/Mo multilayer showed peaks like the Mo thin film deposited on Cu substrate.

The direct structure of the Si/Mo multilayer was obtained by a cross-sectional TEM. Figure 2 shows the stacking sequence of the multilayer deposited on Cu foil: Si 27nm/Mo 3nm/Si27nm/Mo3nm/. . ./Si27nm/Mo 20nm. It was made up of 120 Si/Mo periods. To avoid chemical contamination, especially the native oxidation of Si, the samples were protected by a Mo top layer. The light contrasted areas correspond to Si layers and the dark areas correspond to Mo layers.

Figure 3 shows the initial charge-discharge behaviors of the Si thin film and the multilayer electrodes between 0.01 V and 1,0 V vs. Li/Li$^+$ at a current density of 0.55 mA/cm^2. The effect of Si/Mo atomic ratio on battery performance was further investigated by controlling the thickness of the Mo layer in the deposition time. The multilayer (b) having about 3nm Mo layer and multilayer (c) having about 10nm Mo layer had the Si/Mo atomic ratio of 6.2:1 and 2.0:1, respectively. In the initial discharge, the potential drops rapidly to 0.23∼0.21 V, and then decreases to 0.01V gradually. The multilayer had a lower plateau than Si thin film

due to the resistance caused by the hindrance of lithium insertion. In the all electrodes, approximately 80% discharge capacity was obtained at the low voltage range below 0.6 V. There are no well-defined plateaus corresponding to some specific phase transformations. The first irreversible capacity losses of the three electrodes were (a) 13.3%, (b) 12.6%, and (c) 14.2%, respectively. After the first cycle, the reversible charge-discharge reactions had been maintained and the coulombic efficiency led to a neat 100% for the subsequent cycles. Si thin film and multilayer (b) having the same amount of Si showed similar charge/discharge capacities of 3100/2700 mAh/g corresponding to the reaction of $Li_{3.2}Si$, respectively. In the case of the multilayer (c) containing a relatively larger amount of Mo, however, the Mo sublayer may act not as a buffer layer of Si volume change but as a barrier to lithium transfer. Thus, it showed lower charge/discharge capacities than multilayer (b) in spite of containing the same amount of Si.

To see the electrochemical behavior of the Si/Mo multilayer during lithium insertion/removal in detail, differential capacity (dQ/dV) plots of Si thin film and Si/Mo multilayer were compared in Fig. 4. At the first cycle, the DCP of multilayer showed a similar profile to that of Si thin film. A sharp peak at 0.28V during the first insertion of lithium was associated with the SEI formation. Thus, the reason why the peak of multilayer at 0.28 V is relatively lower than that of Si thin film may be related to the role of the Mo top layer due to the inert reaction with an electrolyte. The onset of a Li-Si reaction at low voltage, which is attributed to the polarization due to kinetic limitations, is also observed as the results of research by of Kumta *et al.* [19]. The shapes of DCP during subsequent cycles were reversible, as shown in Figure 4b.

4. Conclusion

A Si/Mo multilayer was deposited sequentially by rf/dc magnetron sputter. Before the deposition of thin film, a plasma pre treatment for the surface cleaning of current collector was performed. The interface mixing and the enhancement of the contact area with deposited film due to the surface roughness of current collector helped the films acquire advanced adhesion with a current collector, and prevent electrical contact loss. It is considered that the superior capacity retention of the multilayer would be attributed to the presence of Mo. The Mo layer between two Si layers effectively buffered the volume change in the electrode during cycling.

∗ Corresponding Author: e-mail : jwpark@hanyang.ac.kr, Tel : +82-2-2220-0386, Fax: +82-2-2298-2850

1. T. Ohzuku, Y. Iwakashi, and K. Sawai, *J. Electrochem. Soc.* **140** (1993) 2490.

2. S. Megahed and B. Scrosati, *J. Power Sources* **51** (1994) 79.

3. C.J. Wen and R.A. Huggins, *J. Solid State Chem.* **37** (1976) 271.

4. J.O. Besenhard, J. Yang, and M. Winter, *J. Power Sources* **68** (1997) 87.

5. B.A. Boukamp, G.C. Lesh, and R.A. Huggins, *J. Electrochem. Soc.* **128** (1981) 725.

6. R.A. Huggins and B.A. Boukamp, *US patent* #4,436,796 (1984).

7. J. Yang, M. Winter, and J.O. Besenhard, *Solid State Ionics* **90** (1996) 281.

8. W.J. Weydanz, M. Wohlfahrt-Mehrens, and R.A. Huggins, *J. Power Sources* **81-82** (1997) 237.

9. G.X. Wang *et al.*, *J. Power Sources* **88** (2000) 278.

10. Il-seok Kim, P.N. Kumta, and G.E. Blomgren, *Electrochem. Solid-State Lett.* **3** (2000) 493.

11. H. Kim, J. Choi, H.-J. Sohn, and T. Kang, *J. Electrochem. Soc.* **14** (1999) 4401.

12. T. Moriga, K. Watanabe, D. Tsuji, S. Massaki, and L. Nakabayahsi, *J. Solid State Chem.* **153** (2000) 386.

13. G.A. Roberts, E.J. Cairns, and J.A. Reimers, *J. Power Sources* **110** (2002) 424.

14. M. Yoshio *et al.*, *J. Electrochem. Soc. A* **149** (2002) 1598.

15. J.R. Dahn *et al.*, *Thin Solid Films* **111** (2002) 408.

16. Y.-L. Kim *et al.*, *Electrochimica Acta* **00** (2003) 1.

17. K.L. Lee, J.Y. Jung, S.W. Lee, H.S. Moon, and J.W. Park, *J. Power Sources* **129** (2004) 270.

18. T. Motooka and O.W. Holland, *Appl. Phys. Lett.* **58** (1991) 2360; *Electrochem. Solid-state lett. A* **6** (2003) 198.

19. Tsutomu Takamura, Shigeki Ohara, Makiko Uehara, and Junji Suzuki, Kyoichi Sekine, *J. Power Sources* **129** (2004) 96.

20. R.A. Huggins, *J. Power Sources* **81-82** (1999) 13.

21. J.O. Besenhard, J. Yang, and M. Winter, *J. Power Sources* **68** (1997) 87.